Verifying Marine-Hydro-Kinetic Energy Generation Simulations Using SNL-EFDC

Scott C. James
Sandia National Laboratories
Thermal/Fluid Science & Engineering
Livermore, USA
scjames@sandia.gov

Sophia Lefantzi
Sandia National Laboratories
Computer Software Research & Development
Livermore, USA
slefant@sandia.gov

Janet Barco, Erick Johnson, Jesse D. Roberts
Sandia National Laboratories
Water Power Technologies
Albuquerque, USA
jbarcom@sandia.gov, ejohns1@sandia.gov,
jdrober@sandia.gov

***Abstract*—Increasing interest in marine hydrokinetic (MHK) energy has led to significant research regarding optimal placement of emerging technologies to maximize energy capture and minimize effects on the marine environment. Understanding the changes to the near- and far-field hydrodynamics is necessary to assess optimal placement. MHK projects will convert energy (momentum) from the system, altering water velocities and potentially water quality and sediment transport as well. Maximum site efficiency for MHK power projects must balance with the requirement of avoiding environmental harm.**

This study is based on previous modification to an existing flow, sediment dynamics, and water-quality code (SNL-EFDC) where a simulation of an experimental flume is used to qualify, quantify, and visualize the influence of MHK energy generation. Turbulence and device parameters are calibrated against wake data from a flume experiment out of the University of Southampton (L. Myers and A. S. Bahaj, "Near wake properties of horizontal axis marine current turbines," in *Proceedings of the 8th European Wave and Tidal Energy Conference*, 2009, pp. 558-565) to produce verified simulations of MHK-device energy removal. To achieve a realistic velocity deficit within the wake of the device, parametric studies using the nonlinear, model-independent, parameter estimators PEST and DAKOTA were compared to determine parameter sensitivities and optimal values for various constants in the flow and turbulence closure equations. The sensitivity analyses revealed that the Smagorinski subgrid-scale horizontal momentum diffusion constant and the k-ε kinetic energy dissipation rate constant ($C_{\varepsilon 4}$) were the two most important parameters influencing wake profile and dissipation at 10 or more device diameters downstream as they strongly influence how the wake mixes with the bulk flow. These results verify the model, which can now be used to perform MHK-array distribution and optimization studies.

Keywords-MHK simulation, EFDC, model calibration, MHK wake

I. INTRODUCTION

Effective and efficient renewable power generation is a growing global priority given that the world's power usage is expected to increase by more than 70% over the next 30 years due to both population growth and accelerated industrialization [1]. Fossil fuels are the de facto source of energy, but with their use come consequences. Moreover, rapid depletion of these fossil-fuel resources is a growing concern, not to mention that increased atmospheric CO_2 concentrations contribute to climate change. These issues focus increasing attention upon renewable energy as a global solution to both energy and environmental challenges.

Renewable energy sources such as wind power, solar power, and hydroelectric dams are successfully implemented with a high level of efficiency. Nevertheless, the weather dependence and transmission costs (many suitable sites are not collocated with population centers) of wind and solar power installations pose significant challenges. Hydroelectric dams, while quite efficient, may have unforeseen ecological consequences, and more dams are being removed than built in the United States [2]. Recently, marine hydrokinetic (MHK) devices (e.g., water turbines and wave energy converters) are being considered as a practical and effective solution to power generation with reasonable cost, increased predictability, and less intrusion on the environment compared to other, more traditional, power systems. Also, because MHK technology has yet to be widely implemented, there is a high availability and low exploitation of suitable sites. Moreover, MHK installations can be located near population centers (e.g., Cook Inlet near Anchorage, Alaska; Puget Sound near Seattle, Washington; the Hawaiian Islands, the California coast), which will help control transmission costs.

II. Marine Hydrokinetic Considerations

A. Ecological Considerations

While MHK devices hold promise, significant research is needed to quantify and understand their potential environmental effects (both beneficial and potentially harmful). When MHK devices generate energy from a system, volumetric flows and tidal ranges can be affected [3]. In conjunction, sediment dynamics can be altered, changing both erosion/deposition regimes and the size and composition of eroded particles [4]. Because water circulation patterns may change, residence times (flushing rates) may also change, potentially changing algae growth patterns as well as concentrations of nutrients and dissolved gasses [5]. Acoustic energy and electromagnetic waves emanating from MHK devices and infrastructure may perturb wildlife behavior [6, 7]. Holistically, these factors may modify biological dynamics, intrude upon migration paths, disturb life cycles and communication, or alter resource availability. On the other hand, MHK installations can benefit aquatic life by providing shelter and food resources through a reef-like presence or by having the area designated as a marine sanctuary thereby minimizing the otherwise intrusive effects of commercial and recreational shipping activities in that marine environment.

B. Economic Considerations

The economic cost and benefit of MHK installations must also be carefully considered. MHK devices may cost significantly more to install and maintain than their land-based counterparts. Mooring MHK devices in high-velocity and possibly saline waters can add significant expense because those devices must be ruggedized to such conditions. As many MHK devices are most effective for flow velocities in excess of 2 m/s, the viability of installing in slower waters must be considered [8]. Although some technologies may be appropriate for slowly moving flows, such waterways have commensurately low power densities; recall that the power in a fluid scales with the velocity cubed [9]. Also, the benefit of economies of scale must be weighed against diminishing levels of return per turbine as more are installed [3]. The overall efficiency of an MHK installation, coupled with power generation viability and total cost, are covariant concerns.

III. Marine Hydrokinetic Modeling

This effort applies Sandia National Laboratories Environmental Fluid Dynamics Code (SNL-EFDC) to a laboratory flume where an MHK turbine is emplaced. SNL-EFDC is an upgraded version of US Environmental Protection Agency's (EPA's) environmental flow and transport code, Environmental Fluid Dynamics Code (EFDC) [10-13], coupled to both the US Army Corps of Engineers' (ACE's) water-quality code, CE-QUAL-ICM (Quality Integrated Compartment Model) [14, 15], and the sediment dynamics code, SEDZLJ (Sediment, Ziegler, Lick, and Jones) [16-19]. A new module considers energy removal by current-based devices (not wave energy converters) with commensurate changes to the turbulent kinetic energy and the turbulent kinetic energy dissipation rate. One intent of this study is to provide a design tool that is capable of predicting power output from an MHK array configuration using large-scale modeling; it is not intended to provide high-fidelity simulations – computational fluid dynamics (CFD) would be appropriate here. Advantages of using a large-scale model are to: (1) provide a rapid turnaround of simulations that can yield multiple results for the same computational cost as a CFD simulation; and, (2) investigate large-scale environmental effects (e.g., flow characteristics, sediment transport, and water quality). The code was developed for river-, estuary-, and open-ocean-scale systems and never designed with specific consideration for simulating small (flume-scale) systems. Hence, in this application SNL-EFDC is up against its lower scale limit because numerical dispersion, although not dominant, approaches the same order of magnitude as the momentum and turbulence diffusion in the flume-scale study simulated here.

A. EFDC

EFDC was selected over other models of flow and transport in rivers, lakes, and estuaries because it is an open-source, 3D flow and transport code that directly couples sediment-transport and water-quality calculations. It has been successfully applied at numerous sites [20-25] and is sponsored by the US EPA and maintained by its original author, John Hamrick, now with Tetra Tech. There is some precedent for modeling laboratory experiments [17, 26].

The hydrodynamic portion of the model solves the hydrostatic, free surface, Reynolds-averaged Navier-Stokes equations with turbulence closure, similar to the model of Johnson et al. [27]. The numerical solution techniques are the same as those of Blumberg and Mellor [28], except for the solution of the free surface, which is implemented with a preconditioned conjugate gradient (direct) solver rather than an alternating-direction implicit method. EFDC, like many atmospheric and oceanic models, uses a stretched or sigma (σ) coordinate system [29]. That is, it allows a curvilinear orthogonal (or Cartesian) grid in the horizontal, but has a specified number of layers in the vertical. Each layer is assigned a constant (often equal) fraction of the flow depth throughout the model domain; the absolute height of each layer changes with the topology of the model domain (i.e., at 10 m depth and 10 layers, each equal σ layer would be 1 m thick, however at 25 m depth each layer would be 2.5 m thick). EFDC's time integration uses a second-order-accurate, three-time-level, finite difference scheme with an internal/external mode splitting procedure to separate the internal shear (or baroclinic mode calculated across each σ layer) from the external free-surface gravity wave (or barotropic mode calculated on the depth average).

B. CE-QUAL-ICM

The CE-QUAL-ICM [30] code is a water-quality model implemented in EFDC that simulates eutrophication kinetics. This finite-volume model computes constituent concentrations in well-mixed cells that can be arranged in arbitrary one-, two-,

or three-dimensional configurations. The water-quality model simulates transient reactions for parameters including dissolved O_2 and CO_2, algae (cyanobacteria, diatoms, and green algae), and various components of carbon, nitrogen, phosphorus, and silica [14, 31]. The authors of this manuscript have successfully applied this model to various systems [32, 33].

C. SNL-EFDC

The newest iteration of SNL-EFDC provides enhancements to sediment dynamics modeling through the SEDZLJ algorithms. Also, it simulates the effects of marine-hydrokinetic-device energy generation.

1) *SEDZLJ*: EFDC's sediment dynamics are enhanced with the SEDZLJ algorithms (named after its authors Ziegler, Lick, and Jones from UC Santa Barbara) [34]. SEDZLJ provides an alternative to EFDC's original sediment-dynamics formulations and provides a unified treatment of sediment transport, as opposed to considering cohesive and noncohesive sediments separately [16, 18, 35]. Because erosion dynamics vary significantly between test sites, SEDZLJ is written to incorporate 3D sediment-bed data collected with the Sediment Erosion with Depth flume (SEDflume) [36]. Furthermore, SEDZLJ considers bed armoring and consolidation, factors that account for decreased erosion rates with time.

2) *Marine Hydrokinetic Simulation:* A new module to SNL-EFDC simulates removal of energy by MHK current devices. Changes are manifest through a reduction in momentum in the model cell where the device is situated along with commensurate changes to turbulent kinetic energy and the turbulent kinetic energy dissipation rate. Source/sink terms, S_Q, S_K, and S_ε, appropriate to each type of MHK device, represent the rate of momentum reduction, net change to turbulent kinetic energy, and the increase in turbulent kinetic energy dissipation rate, respectively [37]. In addition to the effects from the moving portion of the MHK device (i.e., turbine rotor), the effects of affiliated support structures are also considered.

The sink of momentum, S_Q, and sources of kinetic energy, S_k, and its dissipation rate, S_ε, due to a turbine have been added to the Reynolds Averaged Navier Stokes solver in EFDC as [38]:

$$\begin{aligned} S_Q &= \frac{1}{2} C_T A_M \rho U^3, \\ S_k &= \frac{1}{2} C_T A_M \left(\beta_p U^3 - \beta_d U k \right), \\ S_\varepsilon &= C_{\varepsilon 4} \frac{\varepsilon}{k} S_k, \end{aligned} \tag{1}$$

where C_T (−) is the thrust coefficient, ρ (kg/m^3) is the fluid density, U (m/s) is the flow speed, A_M (m^2) is the flow-facing area of the device (support), dimensionless β_p is the fraction of mean flow kinetic energy, k (m^2/s^2), converted to wake-generated k by drag (i.e., a source term in the k budget), dimensionless β_d is the fraction of k dissipated by conversion to kinetic energy in the MHK device (i.e., a sink term in the k budget), and ε (m^2/s^2) is the kinetic energy dissipation rate where $C_{\varepsilon 4}$ is a closure constant. For vegetative canopies, Katul et al. [37] suggest β_p = 1, β_d = 1−5, and $C_{\varepsilon 4}$ = 0.9 while Réthoré et al. [39] suggest β_p = 0.05, β_d = 1.5, and $C_{\varepsilon 4}$ = 1.6 for wind turbines.

IV. Turbine Experiment and Model Setup

Myers and Bahaj [40] measured the flow field in the wake region of a tidal current turbine in the IFREMER circulating water channel at Boulogne-sur-Mer in France. The 18-m-long, 4-m-wide, 2-m-deep water channel flows at 0.8 m/s; the turbine location in the vertical is shown in Figure 1. The rotor diameter is 800 mm with a 114-mm hub/nacelle diameter and the coefficient of thrust was specified as $C_T = 0.77$. Rotor blades are NACA 48XX aerofoil sections that have good lift/drag performances (reduced stall characteristics) at lower Reynolds numbers. The velocity deficit, a non-dimensional number relative to the free-streamflow speed at hub height (U_0) and the wake velocity (U_w), was selected as the metric of interest to investigate and characterize the wake:

$$U_{\text{deficit}} = 1 - \frac{U_w}{U_0}. \tag{2}$$

The velocity deficit, taking into account both the turbine and support structure, declines from about 0.48 at 3 rotor-diameters downstream to about 0.21 at 10 rotor diameters. Other studies indicate 90% wake recovery within 15−20 turbine diameters downstream [41-43].

An SNL-EFDC model was built to simulate the IFREMER turbine experiment (18 m long by 4 m wide by 2 m deep); the Cartesian grid has 20×20 cm^2 cells using 10 sigma layers that yield approximately 20-cm-thick layers. A constant elevation of 2 m was specified at the downstream boundary and a uniform flow of 6.4 m^3/s was specified at the inlet (yielding a depth-averaged flow speed of 0.8 m/s at the outlet). Flume bottom roughness, which was not reported by Myers and Bahaj [40], was specified as 0.1 mm to establish a reasonable velocity profile in the vertical.

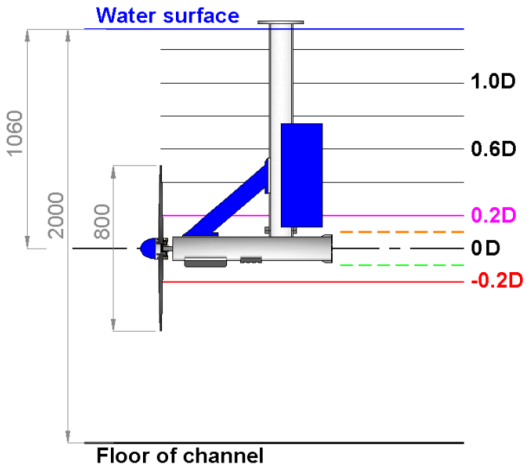

Figure 1: Turbine location in the vertical in the IFREMER circulating water channel [40].

An MHK device and support structure was built into the model to represent the turbine shown in Figure 1 at a location of 6 m downstream from the inlet (to allow time for the vertical velocity profile to develop). Significant efforts were expended to ensure that the difference in total energy (kinetic plus potential) upstream and downstream of the device was equal to the energy converted by the MHK device plus frictional losses to the MHK support structure plus bottom shear-stress losses (for one-, two-, and three-dimensional test problems). The flume sidewalls are specified as frictionless because the cell dimensions are too coarse to adequately capture the boundary layers here.

V. Calibration

A. DAKOTA

DAKOTA (Design Analysis Kit for Optimization and Terascale Applications) is an open-source optimization tool created by Sandia National Laboratories [44]. The DAKOTA optimization tool provides a flexible interface between a simulation code and a variety of iterative methods and strategies, including non-gradient-based algorithms. The model can be used for optimization, uncertainty quantification, and sensitivity analyses.

B. PEST

PEST (Parameter ESTimation) is a nonlinear parameter estimation package. The software is based on a robust implementation of Gauss-Marquardt-Levenberg algorithm, and adjusts the model parameters by weighted least squares. PEST also can be applied for optimization and sensitivity analyses [45-63].

C. Optimization Setup

Given initial parameter guesses (for PEST) and acceptable ranges, DAKOTA and PEST run SNL-EFDC and compare the model output to the wake data from the IFREMER flume. The objective function used is the sum of squared differences between the observed and simulated velocity defect in the wake of the turbine. The parameter estimation tools require template files for the EFDC and MHK inputs and an instruction file to read model output. The adjustable parameters are then replaced with updated estimates that result in a closer match to experimental data. The framework for communication between EFDC and DAKOTA/PEST is shown in Figure 2. Both a genetic algorithm (DAKOTA) and a gradient-based approach (PEST) were investigated. A genetic algorithm is a global minimization strategy while the gradient-based approach sometimes finds a local minimum that can be a function of the initial parameter guesses. The calibration objective function was specified to match the velocity defect at 10 (weight 1) and 15 (weight 2) device diameters downstream where the measured velocity defects there were specified as 0.21 [40] and 0.10 [43], respectively.

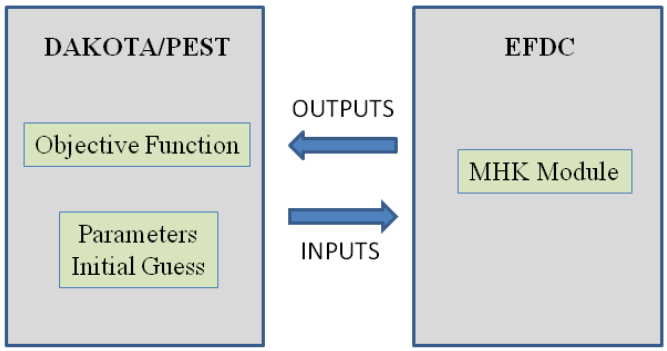

Figure 2: Optimization framework.

VI. Results

The parameters β_p, β_d, $C_{\varepsilon 4}$ in (1) and *ahd* (the dimensionless constant in the Smagorinsky subgrid scale horizontal diffusion formulation [64], which impacts the horizontal momentum diffusivity) were calibrated to optimize the wake characteristics. Initial values were those of Réthoré et al. [39] mentioned above. The wake in the IFREMER flume was fairly persistent, perhaps because of the relatively low level of turbulence intensity (5% in the flume, where 10% might be reasonable in a natural system). Not surprisingly, *ahd* was reduced to a fairly low value because as it increases, the wake is increasingly dispersed. Also, as can be inferred from (1), decreasing $C_{\varepsilon 4}$ tended to increase the wake persistence and the magnitude of the velocity deficit through decreased kinetic energy dissipation rate. Calibrated parameters (and interrogated ranges) are listed in Table 1 and the resulting depth-averaged velocities (using the PEST-calibrated values) are shown in Figure 3.

Table 1: Calibrated model parameters.

Parameter	PEST	DAKOTA	Range
β_p	1.21	2.86	0.01−10
β_d	3.80	31.67	0.5−50
$C_{\varepsilon 4}$	1.82	2.26	0.5−16
ahd	0.10	0.12	0.001−1

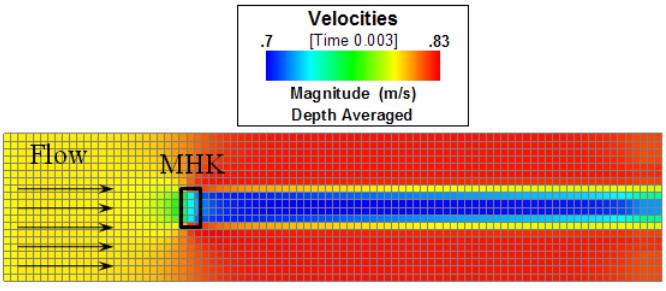

Figure 3: Simulated depth-averaged velocities calibrated to MHK wake data using PEST-estimated parameters.

Note in Table 1 how the DAKOTA parameters are different from those of PEST. DAKOTA's genetic algorithm, which used only 200 evolutions, seeks a global minimum to the objective function without regard for local minima near the initial parameter guesses, which were selected to be consistent

with previous studies with the working fluid being air rather than water [39]. DAKOTA was given broad latitude in searching for this global minimum (see Table 1) and it is not clear that the results are appropriately reflective for the flume system simulated here. The four adjustable parameters and corresponding objective functions as calculated with DAKOTA's genetic algorithm are shown in Figure 4. It is evident that lower values of *ahd* minimize the objective function. In fact, the correlation coefficient between *ahd* and the objective function is quite strong, R^2 = 0.88. The parameters $C_{\varepsilon 4}$, β_p, and β_d seem to be able to fall anywhere in their allowable range without a consistent effect on the objective function (minimal correlation), although one can see how the parameters cluster close to their optimal values near the minimized objective function. Also, when *ahd* increases, $C_{\varepsilon 4}$ decreases because these two parameters trend oppositely to maintain the wake deficit. Aside from β_d, which is the least sensitive parameter in the objective function, the DAKOTA-generated global minimum objective function yields parameters consistent with those from PESTS's gradient-based techniques. Because PEST's minimum objective function was slightly lower than DAKOTA's, its parameters are selected for further study henceforward.

There are also other issues associated with the general approach of using SNL-EFDC (designed for large-scale systems) to simulate the detailed physics present in an experimental flume (which is considered small-scale from the perspective of the model). For example, it is recognized that there will be consequences to globally calibrating the Smagorinsky sub-grid scale coefficient because the overall flow field will be sensitive to it. However, it must be kept in mind that this calibration exercise applies to an experimental flume where flow conditions are fairly uniform and turbulence is less than in a natural system. Thus, results should help provide rough estimates for comparable systems because, as a rule of thumb, the Smakorinsky constant should scale with cell size (a reasonable approximation is about one-one-thousandth of the average cell area in square meters, but in this application, 4×10^{-5} would be far too small a value to use). When velocity deficit data are available from a real turbine in operation, this issue will be visited.

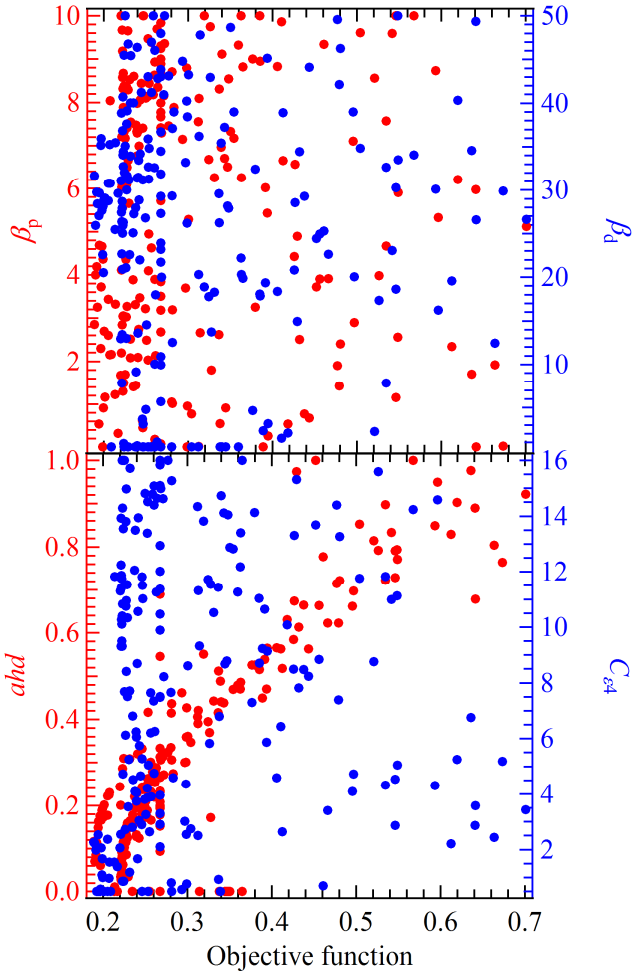

Figure 4: Objective function as a function of the DAKOTA-adjustable parameters.

Parameter sensitivities were also investigated by PEST and by varying them locally and observing the impact on the velocity deficit. In general, the velocity deficit is less sensitive to local variations in β_p and β_d, although it is quite sensitive to *ahd* and $C_{\varepsilon 4}$. Figure 5 shows the trends in velocity deficit at 15 device diameters downstream as a function of percent change in each PEST-estimated model parameter; the trends are consistent with expectations, especially in light of (1). During the calibration exercise, PEST revealed that the k-ε parameters were less sensitive when *ahd* was large because this caused the wake to dissipate quickly. Also, for low *ahd*, $C_{\varepsilon 4}$ was, not surprisingly, quite sensitive. PEST-calculated overall (i.e., not specifically at the minimized objective function) parameter

sensitivities to the objective function are listed in Table 2.

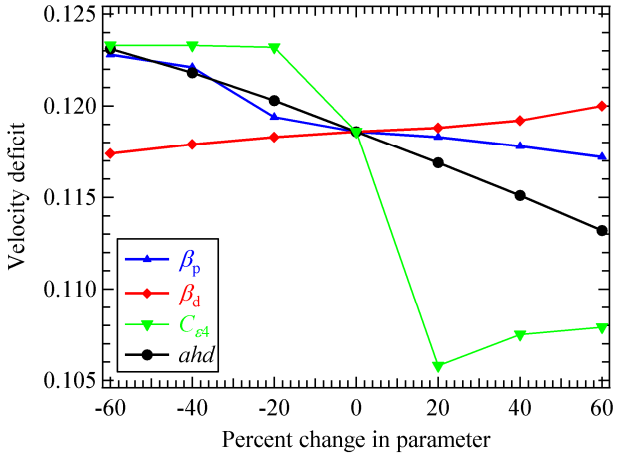

Figure 5: Parameter sensitivity analysis at 15 device diameters downstream.

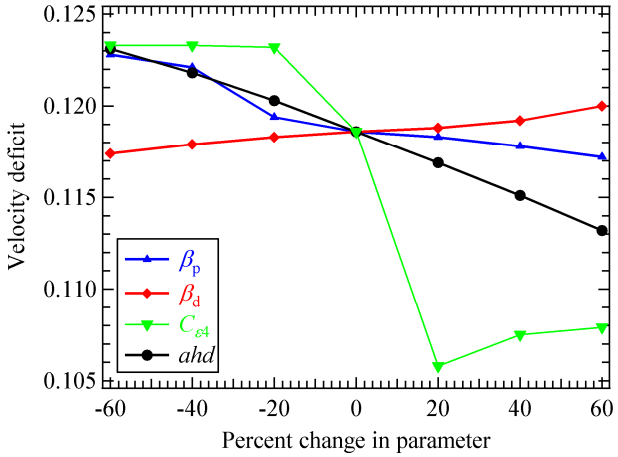

Figure 5: Parameter sensitivity analysis at 15 device diameters downstream.

Table 2: Global parameter sensitivities from PEST.

Parameter	Sensitivity
β_p	0.08
β_d	0.03
$C_{\varepsilon 4}$	0.08
ahd	0.74

VII. DISCUSSION

Myers and Bahaj [40] present their results normalized to two different upstream flows; either the flow without an MHK device present or the flow that results when the device is in place. Differences are due to flow reorganization that occurs even though the device has only a 6.3% blockage ratio and it is not always clear which upstream flow is most appropriate for experimental (and simulated) inter-comparisons. These sorts of issues also arise in the SNL-EFDC simulation where the presence of the device itself alters both upstream and downstream flows. A primary difference between the numerical and physical experiment is that an upstream volumetric flow rate is user-specified in the model and this will be achieved regardless of the presence of the MHK device; this manifests as an increase in upstream elevation with commensurate decrease in downstream water elevation, which yields an increased downstream average velocity (because mass is, of course, conserved). While this may not be intuitive, it is consistent with the concept that much of the MHK power comes from a reduction in the potential energy of the system. Also, the model specifies a constant downstream flow depth as a boundary condition while the experiment has no such constraint. Thus, some discrepancy must be expected because of the inability to exactly replicate the physics of the experiment with SNL-EFDC.

Moreover, it must be kept in mind that SNL-EFDC is designed for large-scale systems and that it is not appropriate for simulating a fine level of detail around (and just downstream of) an MHK device. This is because the effect of the MHK device is distributed across a model cell according to the source/sink calculations of (1) and because the physical displacement of fluid by the device is not simulated [65]. Thus, a fairly large simulated velocity deficit just downstream of the device should not be expected because the MHK device effects are distributed and averaged across each 20-cm cell as if the cell was a porous block [66]. As such, it cannot hope to resolve the fine level of detailed physics involved with an actual device. For example, a real device will have a nacelle at its center and fully block the flow there, but not at the cell edges. EFDC cannot simultaneously represent a momentum sink and block the flow (the entire effect of the turbine is distributed as a representative average across all the cells in which the turbine is assigned present). Increased grid resolution would not remedy this situation because physical fluid displacement through flow blocking is not simulated. Ultimately, the parabolic velocity defect downstream of the device is much flatter in the simulation than in the experiment. Also, Myers and Bahaj [43] state that the velocity deficit at less than 10 device diameters is sufficiently large that placing another turbine in this wake region would produce inefficient amounts of power for practical use. Hence, our goal was not to capture the details of the wake immediately downstream of the device, but to represent its dissipation appropriately at 10 or more MHK diameters downstream. Wake recovery is expected to be faster in natural systems than in flumes because of increased turbulence and cross-mixing. Plans are underway to collect such field data and these data will be used to revisit model calibration when they become available. If these data reveal wake recovery in less than 10 diameters, SNL-EDC could certainly be calibrated to reflect these results.

It should be emphasized, though, that if the data showed, for example 90% wake recovery within 5 device diameters, that the model parameters could be adjusted to accommodate this scenario (most notably by increasing *ahd*). That is, just because SNL-EFDC does not capture the fine-scale physics around and just downstream of an MHK device, it can capture the 90% wake recovery at various downstream distances. This is an important consideration and it implies that SNL-EFDC

can be used to effectively simulate systems with increased turbulence where wakes might recover more quickly. If data are available for such scenarios, corresponding model parameters could be estimated. Overall, the calibration exercise conducted here yields a verified model that can be used to simulate large-scale systems where things like MHK array layout can be optimized and environmental effects minimized.

As a point of order, grid independence was confirmed by sequentially decreasing the spanwise resolution. Maintaining the resolution in the streamwise direction facilitates a direct comparison of the wake. Doubling and quadrupling the grid resolution resulted in the 2×grid being 40×20 cm^2 and a 4×grid of 80×20 cm^2. The optimal PEST parameter values from the original grid were used to test the velocity deficit in the updated grids. However, because the subgrid-scale turbulence should approximately scale with the grid-cell area, *ahd* was scaled to 0.2 and 0.4 respectively (from the original value of 0.1). There was no significant sensitivity to the decrease in grid resolution suggesting that the grid used in this study was appropriately refined.

VIII. Conclusions

SNL-EFDC was used to simulate a flume experiment where the wake characteristics of an 800-mm-diameter MHK device was tested in a 0.8-m/s average flow velocity. Because SNL-EFDC distributes momentum and turbulence effects over a cell and because it does not simulate blockage (physical displacement of fluid by the device), the characteristics of the wake immediately downstream were not sought (SNL-EFDC should be used for a large-scale simulations). For 90% wake recovery SNL-EFDC adequately captures velocity deficit after the Smagorinski subgrid-scale horizontal diffusion constant and the turbulence closure constants were appropriately adjusted using the PEST and DAKOTA calibration packages. This effort is a first step toward extending SNL-EFDC beyond its intended use as a tool to investigate environmental changes into a model that performs array-scale simulations – one that can optimize array design and suggest how to minimize environmental effects.

Acknowledgment

Sandia National Laboratories is a multi-program laboratory managed and operated by Sandia Corporation, a wholly owned subsidiary of Lockheed Martin Corporation, for the U.S. Department of Energy's National Nuclear Security Administration under contract DE-AC04-94AL85000.

References

[1] J. S. Jennings. *Future sustainable energy supply*. in *16th World Energy Council Congress*. 1995. Tokyo, Japan.

[2] G. Cada, J. Ahlgrimm, M. Bahleda, T. Bigford, S. Stavrakas, D. Hall, R. Moursund, and M. Sale, "Potential impacts of hydrokinetic and wave energy conversion technologies on aquatic environments," *Fisheries*. vol. 32(4), 2007.

[3] B. Polagye, M. Kawase, and P. Malte, "In-stream tidal energy potential of Puget Sound, Washington," *Proceedings of the Institution of Mechanical Engineers, Part A: Journal of Power and Energy*. vol. 223(5), pp. 571-587, 2009.

[4] S. P. Neill, E. J. Litt, S. J. Couch, and A. G. Davies, "The impact of tidal stream turbines on large-scale sediment dynamics," *Renewable Energy*. vol. 34(12), pp. 2803-2812, 2009.

[5] DOE, "EISA Report," Department of Energy, Washington, DC, 2009.

[6] Centre for Marine and Coastal Studies, "A baseline assessment of electromagnetic fields generated by offshore windfarm cables," University of Liverpool, Liverpool, England, COWRIE-EMF-01-2002, 2003.

[7] R. Inger, M. J. Attrill, S. Bearhop, A. C. Broderick, W. J. Grecian, D. J. Hodgson, C. Mills, E. Sheehan, S. C. Votier, M. J. Witt, and B. J. Godley, "Marine renewable energy: Potential benefits to biodiversity? An urgent call for research," *Journal of Applied Ecology*. vol. 46, pp. 1145-1153, 2009.

[8] B. L. Polagye, J. Epler, and J. Thomson, "Limits to the predictability of tidal current energy," in *Oceans 2010*, 2010, pp. 1-9.

[9] B. L. Polagye, "Hydrodynamic effects of kinetic power extraction by in-stream tidal turbines," University of Washington, Seattle, WA, 2009.

[10] J. M. Hamrick, "A Three-Dimensional Environmental Fluid Dynamics Computer Code: Theoretical and Computational Aspects," The College of William and Mary, Special Report 317, 1992.

[11] J. M. Hamrick, "User's Manual for the Environmental Fluid Dynamics Computer Code," Virginia Institute of Marine Sciences, Gloucester Point, Virginia, Special Report No. 331, 1996.

[12] J. M. Hamrick, "The Environmental Fluid Dynamics Code: User Manual," US EPA, Fairfax, VA, Version 1.01, 2007.

[13] J. M. Hamrick, "The Environmental Fluid Dynamics Code: Theory and Computation," US EPA, Fairfax, VA, Version 1.01, 2007.

[14] C. F. Cerco and T. Cole, "User's Guide to the CE-QUAL-ICM Three-Dimensional Eutrophication Model, Release Version 1.0," U.S. Army Corps of Engineers, Technical Report EL-95-15, 1995.

[15] K. Park, A. Y. Kuo, J. Shen, and J. M. Hamrick, "A three-dimensional hydrodynamic-eutrophication model (HEM-3D): Description of water quality and sediment process submodels," Virginia Institute of Marine Science, Gloucester Point, Virginia, Special Report in Applied Marine Science and Ocean Engineering No. 327, 1995.

[16] S. C. James, M. D. Grace, M. Ahlmann, C. A. Jones, and J. D. Roberts, "Recent advances in sediment

transport modeling," in *World Environmental and Water Resources Congress*, 2008.

[17] S. C. James, C. A. Jones, M. D. Grace, and J. D. Roberts, "Advances in sediment transport modelling," *Journal of Hydraulic Research*. vol. 48(6), pp. 754 - 763, 2010.

[18] C. A. Jones and W. Lick, "Sediment erosion rates: Their measurement and use in modeling," in *Texas A&M Dredging Seminar*, 2001, pp. 1-15.

[19] W. Lick, Z. Chroneer, C. A. Jones, and R. A. Jepsen, "A predictive model of sediment transport," in *Estaury and Coastal Modeling*, 1998.

[20] J. M. Hamrick, "Analysis of mixing and dilution of process water discharged into the Pamunkey River," Virginia Institute of Marine Science, Gloucester Point, VA, 1991.

[21] J. M. Hamrick, "Estuarine environmental impact assessment using a three-dimensional circulation and transport model," in *Estuarine and Coastal Modeling*, 1992, pp. 292-303.

[22] S. R. Rennie and J. M. Hamrick, "Techniques for visualization of estuarine and coastal flow fields," in *Estuarine and Coastal Modeling*, 1992, pp. 48-55.

[23] J. M. Hamrick, "Linking hydrodynamic and biogeochemical transport models for estuarine and coastal waters," in *Estuarine and Coastal Modeling*, 1993, pp. 591-608.

[24] M. Z. Moustafa and J. M. Hamrick, "Modeling circulation and salinity transport in the Indian River Lagoon," in *Estuarine and Coastal Modeling*, 1993, pp. 381-395.

[25] Z.-G. Ji, J. M. Hamrick, and J. Pagenkopf, "Sediment and metals modeling in shallow river," *Journal of Environmental Engineering*. vol. 128(2), pp. 105-119, 2002.

[26] S. C. James, P. L. Shrestha, and J. D. Roberts, "Modeling noncohesive sediment transport using multiple sediment size classes," *Journal of Coastal Research*. vol. 22(5), pp. 1125-1132, 2006.

[27] B. Johnson, K. Kim, R. Heath, B. Hsieh, and H. Butler, "Validation of three-dimensional hydrodynamic model of Chesapeake Bay," *Journal of Hydraulic Engineering-ASCE*. vol. 119(1), pp. 2-20, 1993.

[28] A. F. Blumberg and G. L. Mellor, *A description of a three-dimensional coastal ocean circulation model*, in *Three Dimensional Coastal Ocean Models*, N. S. Heaps, Editor 1987, American Geophysical Union: Washington, DC. p. 1-16.

[29] J. M. Hamrick, "The Environmental Fluid Dynamics Code: Theory and Computation," US EPA, Fairfax, VA, 2007.

[30] C. F. Cerco. (2010) CE-QUAL-ICM: A Multi-Dimensional, Water Quality Model for Surface Water. [Online]. Available: http://el.erdc.usace.army.mil/elmodels/icminfo.html

[31] T. Wood. (2010) SMIC -- CE-QUAL-ICM Pages. [Online]. Available: http://smig.usgs.gov/SMIC/model_pages/cequalicm.html#abstract

[32] S. C. James, C. Jones, J. D. Roberts, M. Ahlmann, and D. F. Bucaro, "Sediment transport and water quality model of Cedar Lake," in *American Geophysical Union Fall Meeting*, 2006.

[33] S. C. James and V. Boriah, "Modeling algae growth in an open-channel raceway," *Journal of Computational Biology*. vol. 17(7), pp. 895-906, 2010.

[34] C. A. Jones, "A Sediment Transport Model," PhD thesis thesis, University of California Santa Barbara, Santa Barbara, 2001.

[35] P. X. H. Thanh, M. D. Grace, and S. C. James, "Sandia National Laboratories Environmental Fluid Dynamics Code: Sediment Transport User Manual," Sandia National Laboratories, Livermore, CA, SAND2008-5621, 2008.

[36] J. McNeil, C. Taylor, and W. Lick, "Measurement of erosion of undisturbed bottom sediments with depth," *Journal of Hydraulic Engineering-ASCE*. vol. 122(6), pp. 316-324, 1996.

[37] G. G. Katul, L. Mahrt, D. Poggi, and C. Sanz, "One- and two-equation models for canopy turbulence," *Boundary-Layer Meteorology*. vol. 113, pp. 81-109, 2004.

[38] S. C. James, E. Seetho, C. Jones, and J. Roberts. *Simulating environmental changes due to marine hydrokinetic energy installations*. in *OCEANS 2010*. 2010.

[39] P.-E. Rethoré, N. N. Sørensen, and F. Zahle, "Study of the atmospheric wake turbulence of a CFD actuator disc model," in *European Wind Energy Convention*, 2009, pp. 1-9.

[40] L. Myers and A. S. Bahaj, "Near wake properties of horizontal axis marine current turbines," in *Proceedings of the 8th European Wave and Tidal Energy Conference*, 2009, pp. 558-565.

[41] A.-B. S. Bahaj, L. E. Myers, M. D. Thomson, and N. Jorge, "Characterising the wake of a horizontal axis marine turbine," in *7th European Wave and Tidal Energy Conference*, 2007, pp. 1-9.

[42] M. E. Harrison, W. M. J. Batten, L. E. Myers, and A. S. Bahaj, "A comparison between CFD simulations and experiments for predicting the far wake of horizontal axis tidal turbines," in *Proceedings of the 8th European Wave and Tidal Energy Conference*, 2009, pp. 566-575.

[43] L. E. Myers and A. S. Bahaj, "Experimental analysis of the flow field around horizontal axis tidal turbines by use of scale mesh disk rotor simulators," *Ocean Engineering*. vol. 37, pp. 218-227, 2010.

[44] M. S. Eldred, B. M. Adams, D. M. Gay, L. P. Swiler, K. Haskell, W. J. NBohnhoff, J. P. Eddy, W. E. Hart, J.-P. Watson, P. D. Hough, and T. G. Kolda,

"DAKOTA, A multilevel parallel object-oriented framework for design optimization, parameter estimation, uncertainty quantification, and sensitivity analysis," Sandia National Laboratories, Albuquerque, NM, SAND2006-6337, 2006.

[45] S. Christensen and J. D. Doherty, "Predictive error dependencies when using pilot points and singular value decomposition in groundwater model calibration," *Advances in Water Resources*. vol. 31(4), pp. 674-700, 2008.

[46] J. Doherty and D. E. Welter, "A short exploration of structural noise," *Water Resources Research*. vol. 46, pp. W05525, 2010.

[47] J. E. Doherty, "Ground water model calibration using pilot points and regularization," *Ground Water*. vol. 41(2), pp. 8, 2003.

[48] J. E. Doherty, "Addendum to the PEST Manual," Watermark Numerical Computing, Brisbane, Australia, 2010.

[49] J. E. Doherty, "Manual for PEST: Model Independent Parameter Estimation," Watermark Numerical Computing, Brisbane, Australia, 2009.

[50] J. E. Doherty and R. J. Hunt, "Two statistics for evaluating parameter identifiability and error reduction," *Journal of Hydrology*. vol. 366(1-4), pp. 119-127, 2009.

[51] J. E. Doherty and R. J. Hunt, "Two easily-calculated statistics for evaluating parameter identifiability and error reduction," *Journal of Hydrology*. vol. 366, pp. 119-127, 2009.

[52] M. Gallagher and J. E. Doherty, "Predictive error analysis for a water resource management model," *Journal of Hydrology*. vol. 34(3-4), pp. 513-533, 2006.

[53] M. R. Gallagher and J. D. Doherty, "Parameter interdependence and uncertainty induced by lumping in a hydrologic model," *Water Resources Research*. vol. 43, pp. W05421, 2007.

[54] R. Hunt and J. E. Doherty, "Easily-calculated parameter identifiability statistics," 2008.

[55] R. J. Hunt, J. E. Doherty, and M. J. Tonkin, "Are models too simple? Arguments for increased parameterization," *Ground Water*. vol. 45(3), pp. 254-262, 2007.

[56] S. C. James, J. D. Doherty, and A.-A. Eddebbarh, "Practical postcalibration uncertainty analysis: Yucca Mountain, Nevada," *Ground Water*. vol. 47(6), pp. 851-869, 2009.

[57] C. Moore, "The use of regularized inversion in groundwater model calibration and prediction uncertainty analysis," University of Queensland, Brisbane, 2006.

[58] C. Moore and J. E. Doherty, "Role of the calibration process in reducing model predictive error," *Water Resources Research*. vol. 41(5), pp. W05050, 2005.

[59] C. Moore and J. E. Doherty, "The cost of uniqueness in groundwater model calibration," *Advances in Water Resources*. vol. 29(4), pp. 605-623, 2006.

[60] C. Moore, T. Wöhling, and J. Doherty, "Efficient regularization and uncertainty analysis using a global optimization methodology," *Water Resources Research*. vol. 46, pp. W08527, 2010.

[61] M. J. Tonkin and J. E. Doherty, "A hybrid regularized inversion methodology for highly parameterized environmental models," *Water Resources Research*. vol. 41, pp. W10412, 2005.

[62] M. J. Tonkin and J. E. Doherty, "Calibration-constrained Monte Carlo analysis of highly-parameterized models using subspace techniques," *Water Resources Research*. vol. 45, pp. W00B10, 2009.

[63] M. J. Tonkin, J. E. Doherty, and C. Moore, "Efficient nonlinear predictive error variance for highly parameterized models," *Water Resources Research*. vol. 43, pp. W07429, 2007.

[64] J. Smagorinsky, "General circulation experiments with primitive equations 1: The basic experiment," *Monthly Weather Review*. vol. 91(3), pp. 99-164, 1963.

[65] X. Sun, "Numerical and experimental investigation of tidal current energy extraction," Univeristy of Edinburgh, Edinburgh, UK, 2008.

[66] X. Sun, J. P. Chick, and I. G. Bryden, "Laboratory-scale simulation of energy extraction from tidal currents," *Renewable Energy*. vol. 33(6), pp. 1267-1274, 2008.